Concrete Fracture Prediction Using Virtual Internal Bond Model with Modified Morse Functional Potential

Kyoungsoo Park, Glaucio H. Paulino and Jeffery R. Roesler

Department of Civil and Environmental Engineering, University of Illinois at Urbana Champaign, 205N. Mathews Ave. Urbana, IL,61801, U.S.A.

Abstract. Concrete fracture behavior is predicted by one of multi-scaling methods, called the virtual internal bond (VIB) model. The VIB model describes the microscopic interactions between the cement pastes and aggregates using the concept of homogenization. The microscopic behavior is connected to macroscopic behavior by the Cauchy-Born rule, which results in the strain energy function. From the macroscopic strain energy function, the VIB model represents both elastic and fracture behavior within the framework of continuum mechanics. In this study, a modified Morse functional potential is introduced for material particles interactions so that the potential is independent of the length scale lattice parameter. The other parameters in the potential function are determined on the basis of macroscopic fracture parameters, i.e. the fracture energy and the cohesive strength. Moreover, the fracture energy is evaluated in conjunction with the *J*-integral. Finally, the VIB model with the modified Morse potential is verified by the double cantilever beam test and validated by three-point bending tests.

Keywords: Concrete, Virtual Internal Bond Model, Morse Functional Potential.

INTRODUCTION

Classical linear elastic fracture mechanics (LEFM) has limitations to simulate crack initiation and propagation, especially for quasi-brittle materials such as concrete [1]. To characterize a nonlinear fracture process zone, a cohesive surface element [2, 3] is introduced, based on the concept of cohesive zone model. The cohesive surface element describes fracture behavior while the bulk element captures, for example, elastic behavior.

Based on a multiscale interpretation of a cohesive law, a virtual internal bond (VIB) model was presented by Gao and Klein [4, 5]. The VIB model describes the microscopic interactions between particles with the concept of homogenization. The microscopic behaviors are connected to macroscopic behaviors by the Cauchy-Born rule, which results in the strain energy function [6]. Therefore, the VIB model represents both elastic and fracture behaviors within the framework of continuum mechanics. Moreover, Gao and Ji [7] implemented the VIB modeling in nanomaterials illustrating transitions of the fracture mechanism from classical LEFM to one of homogeneous failure near the theoretical strength of solids. Afterwards, Thiagarajan et

CP973, *Multiscale and Functionally Graded Materials 2006*
edited by G. H. Paulino, M.-J. Pindera, R. H. Dodds, Jr., F. A. Rochinha, E. V. Dave, and L. Chen

al. [8] investigated dynamic fracture behavior for a brittle material under impact loading.

This paper investigates fracture behavior of concrete by introducing a modified Morse potential. The potential is independent of a lattice parameter, and represents two basic fracture parameters, i.e. cohesive strength and fracture energy.

THE VIRTUAL INTERNAL BOND (VIB) MODEL

The macroscopic strain energy function is characterized by the bond potential function via the Cauchy-Born rule. Based on the Cauchy-Born rule, continuum behavior is described by a single mapping function, i.e. deformation gradient **F**. Therefore, the bonding potential, $U(\ell)$, is defined by a deformed virtual bond length,

$$\ell = \ell_0 \sqrt{\boldsymbol{\xi} \cdot \mathbf{F}^T \mathbf{F} \boldsymbol{\xi}}, \tag{1}$$

along a bond direction $\boldsymbol{\xi}$, where ℓ_0 is an undeformed virtual bond length. Based on the bonding potential, a strain energy function is represented by the summation of the bonding potential with a bond density, D_Ω, over domain Ω,

$$\Phi = \int U(\ell) D_\Omega d\Omega = \langle U(\ell) \rangle, \tag{2}$$

where $\langle \cdots \rangle = \int \cdots D_\Omega d\Omega$.

In this study, the two dimensional constant bond density function, $D_\Omega = D_0$, is considered, which illustrates an isotropic solid, and has the same initial bond length (ℓ_0) over the domain. The constant bond density function and two dimensional bond direction, $\boldsymbol{\xi} = (\cos\phi, \sin\phi)$, simplify the strain energy function as follows

$$\Phi = D_0 \int_0^{2\pi} U(\ell) d\phi, \tag{3}$$

which is also suitable for the numerical investigation of fracture parameters.

From the determination of the strain energy function (3), the constitutive relation is formulated on the basis of continuum mechanics. The Lagrangian strain, **E**, and the 2nd Piola-Kirchhoff stress tensor, **S**, are used for the calculation of the stress and the material tangential modulus. The derivative of the strain energy with respect to the Lagrangian strain provides the second Piola-Kirchhoff stress,

$$S_{IJ} = \frac{\partial \Phi}{\partial E_{IJ}} = \left\langle \ell_0^{\,2} \frac{U'}{\ell} \xi_I \xi_J \right\rangle, \tag{4}$$

where the superscript prime denotes the derivative with respect to the virtual bond length. The material tangent modulus is obtained by the second derivative of the strain energy function with respect to the Lagrangian strain,

$$C_{IJKL} = \frac{\partial \Phi}{\partial E_{IJ} \partial E_{KL}} = \left\langle \ell_0^{\,4} \left(\frac{U''(\ell)}{\ell^2} - \frac{U'(\ell)}{\ell^3} \right) \xi_I \xi_J \xi_K \xi_L \right\rangle, \tag{5}$$

which satisfies the Cauchy symmetry, $C_{IJKL} = C_{IKJL}$, as well as the usual major and minor symmetries of elasticity. Because of these symmetries, only one elastic property is necessary. Therefore, the Cauchy symmetry is satisfied by the fourth order isotropic elasticity tensor whose Lamé parameters (μ, λ) are the same [8].

Virtual Bond Potential: Modified Morse Potential

The focus of the VIB model is the determination of the virtual bond potential $U(l)$. Previous researchers [4, 5, 8, 9, 10] have utilized the two-parameter phenomenological cohesive law,

$$U'(\ell) = A(\ell - \ell_0)\exp(-(\ell - \ell_0)/B), \tag{6}$$

for the bonding potential. The constant A is related to the initial Young's modulus while the constant B can be determined by the cohesive strength or by the fracture energy. Thus, this potential function can only characterize the initial elastic properties and one fracture parameter.

This study modifies the generalized Morse potential proposed by Milstein [11], an atomistic pair bond potential, so that the proposed potential is independent of the initial bond length, and characterizes two fracture parameters, i.e. the fracture energy and the cohesive strength. Additionally, the modified Morse potential satisfies the general physical properties of an atomistic potential stated by Girifalco and Weizer [12]. The modified Morse functional potential is expressed as

$$U(\ell) = \frac{1}{m-1}\left[\exp(-m\alpha(\ell/\ell_0 - 1)) - m\exp(-\alpha(\ell/\ell_0 - 1))\right] \tag{7}$$

so that the potential function is independent of the lattice parameter (ℓ_0) because the particle distance (ℓ) is normalized with respect to the lattice parameter. However, the Morse potential by Milstein [11] is dependent on the lattice parameter. The two exponents (m, α) in the potential characterize two fracture parameters: the cohesive strength and the fracture energy.

Elastic Properties at Infinitesimal Strains

Elastic material properties of the VIB model are evaluated at the state of small strain by defining the material tangential modulus in two different ways [4]. Either the strain energy function (3) of the VIB model or the linear elastic strain energy function represents the material tangential modulus. Then, from the Cauchy symmetry relation, by equating the tangential modulus from the strain energy function of the VIB model with the tangential modulus from the linear elastic strain energy function, one obtains the relationship between the shear modulus (μ) and the bond potential,

$$\mu = \frac{\pi}{4}\ell_0^2 D_0 U''(\ell_0), \tag{8}$$

for a two dimensional problem. The elastic properties are also represented by the Poisson's ratio (ν) and Young's modulus (E) whose relationship is

$$\nu = \frac{1}{3} \text{ and } E = \frac{2\pi}{3}\ell_0^2 D_0 U''(\ell_0). \tag{9}$$

Elastic Fracture Properties and Mesh Dependence

The essential fracture characteristic of the VIB model is that the fracture energy depends on the element size [13], which can be explained by the path independent J-integral [14]. Because of the path independence, a contour is selected along the upper and lower bound of a localization zone (h_L) where stress softening occurs for a mode I

fracture [13]. The selected contour results in the symmetric stress and displacement field, and then we obtain J for mode I,

$$J = h_L \int_1^{\infty} P_{22} d\lambda_2 = G_I \tag{10}$$

where P_{22} is the 1st Piola-Kirchhoff stress along the x_2 direction. Therefore, the J-integral introduces a length scale (h_L) which is proportional to the fracture energy.

Moreover, because the fracture energy depends on the localization zone size (h_L), which is related to the VIB element size, the reference fracture energy (G_{F0}) is defined as corresponding to the reference localization zone size (h_{L0}). If the size of the localization zone (h_L) grows in the finite element mesh, the numerical result of the fracture energy (G_F) also increases with the same ratio as that of the localization zone.

NUMERICAL VERIFICATION AND VALIDATION

Numerical simulations of the VIB model are implemented by using a commercial software, i.e. ABAQUS, with the application of the user material (UMAT) subroutine capability. In this section, the element size dependence is verified by simulating the double cantilever beam (DCB) test. Furthermore, the VIB model is validated with the three-point bending (TPB) tests of Roesler et al. [15].

Verification of Fracture Properties and Element Size Dependence

The numerical simulations of the DCB test verify the relationship between the fracture energy and the size of the localization zone, derived by the J-integral, because the DCB test provides the analytical solution of the energy release rate. The DCB geometry has an initial notch (a_0) of 0.1 m, height ($2h$) of 0.1m, and length (L) of 1 m. The localization zone is defined by the VIB element along the direction of crack propagation. The exponents (m, α) in the bond potential are determined by numerical simulations of the pure tension test with the reference localization zone size (h_{L0} = 0.0005m) because numerical results of the test provide the cohesive strength and the fracture energy. The peak stress corresponds to the cohesive strength (f_t' = 4.15 MPa). The fracture energy of numerical results is the area under the stress-displacement curve (G_{F0} =164N/m). Additionally, the bond density is calculated by the equation (9) with the initial Young's modulus of 32GPa.

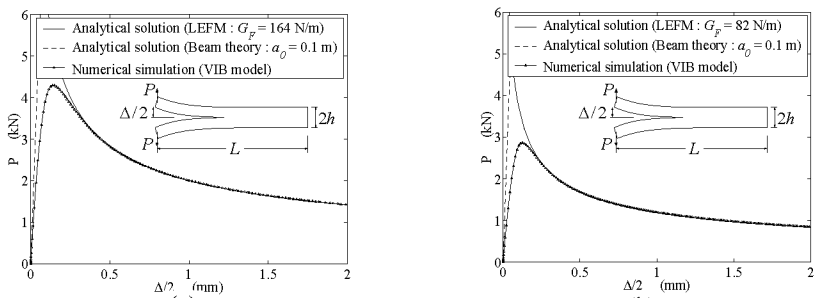

FIGURE 1. Numerical simulation results of DCB test using the VIB model with the localization zone size, (a) h_L = 0.0005m and (b) h_L=0.00025m.

The numerical simulations of the DCB are implemented with two different VIB element sizes (h_L = 0.0005m, 0.00025m), with the same geometry and with the same constants in the bond potential. For the size of 0.0005m, the numerical result is plotted in Figure 1(a) with the LEFM analytical solution whose fracture energy is 164 N/m. Figure 1(b) illustrates the agreement of the numerical result and the analytical solution. The localization zone size is 0.00025m for the numerical simulation and the fracture energy is 82 N/m for the analytical solution of LEFM. These numerical results illustrate that the fracture energy is proportional to the localization zone size.

Experimental Validation: Three-Point Bending Tests

In order to validate the VIB model for concrete, the authors compare numerical results with the previous experimental results from the TPB tests, performed by Roesler et al. [15]. The geometry of the specimens is described in Figure 2, and experimental elastic and fracture properties are presented in Table 1.

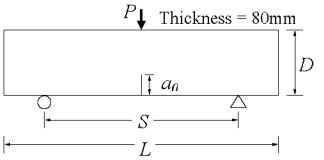

D (mm)	L (mm)	S (mm)	a_0 (mm)
63	350	250	21
150	700	600	50
250	1100	1000	83

FIGURE 2. Geometry of specimens

Based on the concrete properties, the constants in the modified Morse potential are evaluated by the numerical simulations of the pure tension test with the localization zone size of 0.5mm. Table 1 illustrates the calculated constants in the bonding potential. The exponent m increases with respect to the size. This is because the increase of specimen size produces larger total fracture energy with the fixed cohesive strength, which results in the shallow long-range potential. Moreover, this feature corresponds to the characteristics of the Morse potential; a larger value of m results in the longer range of the potential [11]. Figures 3 (a), (b) and (c) illustrate the correspondence between the numerical predictions of the VIB model and the experimental results for each specimen size with respect to the normalized load versus crack mouth opening displacement (CMOD) curves ($P/tD\,f_t'$ − CMOD f_t'/G_F).

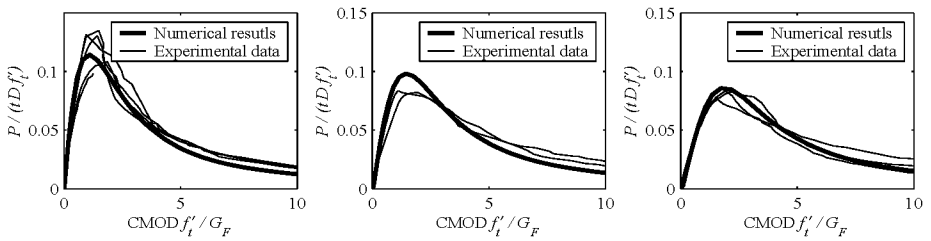

FIGURE 3. Numerical predictions of load-CMOD curves compared with experimental data: (a) specimen size D = 63mm, (b) specimen size D = 150mm, and (c) specimen size D = 250mm

TABLE 1. Material properties of each size of beam and the exponents in the bond potential with the localization zone size of 0.5mm

D (mm)	E (GPa)	f_t' (MPa)	G_F(N/m)	α	m
63			119	34	315
150	32	4.15	164	23	480
250			167	22	510

CONCLUSION

The modified Morse potential is proposed for the bond potential in the VIB model. The modified potential function is independent of the lattice parameter (ℓ_0), and the VIB model characterizes both elastic and fracture behaviors. The elastic modulus, cohesive strength and fracture energy, which can be experimentally obtained, determine the bond density function and the modified Morse potential. The elastic modulus is associated with the bond density; and the cohesive strength and the fracture energy are evaluated by numerical simulations in conjunction with the localization zone size. The numerical simulation of the DCB test verifies that the fracture energy is proportional to the localization zone size for mode I fracture. In addition, the VIB model is validated by predicting the load-CMOD curves of TPB experimental tests. The model parameters in the bond density potential are estimated by the experimental fracture parameters without any calibration. The numerical results of the VIB model correspond to the experimental data. Furthermore, the present framework could be extended to account for other physical interactions, e.g. friction or fiber bridging.

ACKNOWLEDGMENT

This study was supported by the Center of Excellence for Airport Technology, funded by the Federal Aviation Administration under Research Grant Number 95-C-001, and the University of Illinois at Urbana-Champaign (UIUC).

REFERENCES

1. Z. P. Bazant, *Fracture Mechanics of Concrete: Structural Application and Numerical Calculation*, 1-49 (1985).
2. X. P. Xu and A. Needleman, *Journal of the Mechanics and Physics of Solids,* **42**, 1397-1434 (1994).
3. G. T. Camacho and M. Ortiz, *International Journal of Solids and Structures,* **33**, 2899-2938 (1996).
4. H. Gao and P. Klein, *Journal of the Mechanics and Physics of Solids,* **46**, 187-218 (1998).
5. P. Klein and H. Gao, *Engineering Fracture Mechanics,* **61**, 21-48 (1998).
6. E. B. Tadmor, M. Ortiz and R. Phillips, *Philosophical Magazine A,* **73**, 1529-1563, (1996).
7. H. Gao and B. Ji, *Engineering Fracture Mechanics,* **70**, 1777-1791 (2003).
8. G. Thiagarajan, K. J. Hsia and Y. Huang, *Engineering Fracture Mechanics,* **71**, 401-423 (2004).
9. T. D. Nguyen, S. Govindjee, P. A. Klein and H. Gao, *Computer Methods in Applied Mechanics and Engineering,* **193**, 3239-3265 (2004).
10. P. Zhang, P. Klein, Y. Huang, H. Gao and P. D. Wu, *Computer Modeling in Engineering & Sciences,* **3**, 263-277 (2002).
11. F. Milstein, *Journal of Applied Physics,* **44**, 3825-3832 (1973).
12. L. A. Girifalco and V. G. Weizer, *Physical Review,* **114**, 687-690 (1959).
13. P. A. Klein, J. W. Foulk, E. P. Chen, S. A. Wimmer and H. Gao, *Theoretical and Applied Fracture Mechanics,* **37**, 99-166 (2001).
14. J. R. Rice, *Journal of Applied Mechanics,* **35**, 379-386 (1968).
15. J. R. Roesler, G. H. Paulino, K. Park, and C. Gaedicke, *Cement and Concrete Composites,* **29**, 300-312 (2007).